

Supporting Information

A Fe-thiolate layered metal organic framework as a high-performance electrode material for potassium-ion batteries

Long H.B. Nguyen,^{ad†} Pablo Salcedo-Abraira,^{b†} Dat Le Thanh,^{ae} Nusik Gedikoglu,^a
Nathalie Guillou,^c Robin Coatleven,^a Philippe Poizot,^b Fabrice Salles,^a Nicolas Louvain,^{ad}
Lorenzo Stievano^{ad*} and Thomas Devic^{b*}

^a ICGM, Univ. Montpellier, CNRS, ENSCM, Montpellier, France. E-mail: lorenzo.stievano@umontpellier.fr

^b Nantes Université, CNRS, Institut des Matériaux de Nantes Jean Rouxel, IMN, F-44000 Nantes, France. E-mail: thomas.devic@cnrs-imn.fr

^c Institut Lavoisier de Versailles, UMR CNRS 8180, Université de Versailles St-Quentin en Yvelines, Université Paris Saclay, 78035 Versailles, France.

^d Réseau sur le Stockage Electrochimique de l'Energie (RS2E), FR CNRS 3459, Amiens, France

^e Institut Laue-Langevin (ILL), 38042, Grenoble, France

† These authors contributed equally.

Experimental part

1. Synthesis

2,5-disulfhydrylbenzene-1,4-dicarboxylic acid (H_4DSBDC) was synthesized based on the procedure published by Vial et al.¹ The preparation of $K\{Fe(DSBDC)\}\cdot 3H_2O$ was slightly modified compared to our previous report.² 50 mg of H_4DSBDC (0.217 mmol) were dissolved in 1 mL of DMF. By other hand, 58.7 mg (0.217 mmol) of $FeCl_3\cdot 6H_2O$ were dissolved in 1 mL of DMF. Both solutions were mixed in a 23 mL Teflon-lined reactor, and 2.565 mL of DMF were added. Upon mixing, an immediate change of colour from yellowish to dark-green is observed. 0.434 mL of a 1 M aqueous solution of KOH (0.434 mmol) were added dropwise under stirring. The reactor was then closed and heated at 180 °C for 17 hours. The resulting black powder was recovered by filtration, washed with DMF, water and EtOH and dried under air. $K\{Fe(DSBDC)\}$ was prepared by heating $K\{Fe(DSBDC)\}\cdot 3H_2O$ at 150°C under vacuum for one night.

2. X-ray diffraction

Crystal structures of $K\{Fe(DSBDC)\}\cdot 3H_2O$ and $K\{Fe(DSBDC)\}$ were elucidated from powder X-ray diffraction (PXRD) data collected on the CRISTAL beamline at Synchrotron SOLEIL (L'Orme des Merisiers, France). Extractions of the peak positions, pattern indexing, whole powder pattern decomposition, structural determination (simulated annealing and difference Fourier calculations), as well as Rietveld refinement were carried out with the TOPAS program.³ For $K\{Fe(DSBDC)\}\cdot 3H_2O$, the LSI-indexing method converged to a triclinic unit cell similar to that of $Na\{Fe(DSBDC)\}\cdot 2.5H_2O$ ($M_{20} = 18$, see Table S1), suggesting that the two phases were isostructural. The framework of $Na\{Fe(DSBDC)\}\cdot 2.5H_2O$ was then used as the starting point for the structural investigation of the as-synthesized phase, for which the DSBDC ligand was treated as rigid body. In order to achieve greater flexibility of the carboxylate functions and consistent K-O distances, the model was refined in the $P1$ space group and difference Fourier calculations allowed to locate additional water molecules. Due to the lower quality of the data, which show broader peaks, indexing of the anhydrous phase was undertaken using the LP-search method, which avoids difficulties associated with precise peak positions extraction. The framework of the hydrated phase was used as the starting point and the noncentric space group was preserved, even if the the structure could have been refined in $P-1$. At their final stage, the Rietveld plots (Figures S1 and S2) correspond to satisfactory model indicators and profile factors (see Table S1). CCDC- 2448040, and CCDC- 2448041 contain the supplementary crystallographic data for $K\{Fe(DSBDC)\}\cdot 3H_2O$ and

K{Fe(DSBDC)}, respectively. These data can be obtained free of charge from the Cambridge Crystallographic Data Centre via <http://www.ccdc.cam.ac.uk/Community/Requestastructure>. Attempts to index diffraction pattern of the intermediate phase were also undertaken and lead to a triclinic unit cell whose volume is on average twice that of the as-synthesized/anhydrous compounds ($a = 3.604$, $b = 8.708$, $c = 17.811$ Å, $\alpha = 102.336$, $\beta = 89.888$, $\gamma = 98.169^\circ$, $V = 540.20$ Å³, with $M_{15} = 21$). Due to the complexity of this unit cell and the broadening of the diffraction peaks, it was impossible to confirm it with a whole profile analysis of the diffraction pattern. Nevertheless, it is interesting to note that the a and b parameters are preserved, suggesting a superstructure for this intermediate compound.

Routine room temperature PXRD patterns were collected either in a Bragg-Brentano mode (flat sample holder) with a Bruker D8 Advance diffractometer, or in a Debye-Scherrer mode (sealed glass capillary) with an INEL XRG3500 diffractometer, both equipped with a Cu anode. Variable temperature PXRD experiments were carried both under air and dry nitrogen using an Anton Paar XRK 900 high-temperature chamber in a Bruker D8 Advance diffractometer collecting each 10 °C with a heating rate of 1 °C·min⁻¹.

Operando synchrotron PXRD experiments were carried out in transmission mode at the MCX beamline of synchrotron Elettra (Trieste, Italy), using a previously described Leriche-type electrochemical cell.⁴ The preparation of self-supported electrodes and cell assembling protocols followed procedures similar to those described later in section “4 – Electrochemistry” of the Supporting Information. Each electrode contained approximately 8 mg of active material. To avoid X-ray attenuation by highly absorbing potassium metal, a hole was made in the centre of the potassium counter electrode. Data were collected at $\lambda = 0.6889$ Å in the transmission mode in the 2θ range 2.0–29.2°. *Operando* data were acquired during the first discharge and first charge in various conditions: C/20 and C/2 for K{Fe(DSBDC)} vs. K cells, and C/5 for K{Fe(DSBDC)} vs. Li cell. In all three cells, a 30-minute voltage hold was applied at the end of discharge and charge to promote complete phase transition and reach the equilibrium. The backgrounds of the obtained PXRD patterns were subtracted using the same background function to clearly observe the evolution of peak position, variation in peak intensity or broadening, as well as peak appearance or disappearance during cycling.

3. Mössbauer spectrometry

Transmission ⁵⁷Fe Mössbauer spectra were collected at room temperature with a triangular velocity waveform. A Kr gas-filled proportional counter was used for the detection of the γ -rays produced by a 0.5 GBq ⁵⁷Co:Rh source, kept at room temperature. Velocity calibration

was performed with an α -Fe foil at room temperature. Absorbers containing $\sim 20 \text{ mg cm}^{-2}$ of active material were used in all acquisitions. Isomer shifts are referred to α -Fe at room temperature.

In situ Mössbauer measurements were carried out by galvanostatic cycling a self-supported electrode of dehydrated $\text{K}\{\text{Fe}(\text{DSBDC})\}$ vs. K metal at C/50 in the potential range 1,8-3.1 V vs K^+/K in a Leriche-type electrochemical cell.⁴ Spectra were measured at fixed voltages, which were held constant during the acquisition.

The spectra were analysed using appropriate combinations of quadrupole doublets with Lorentzian profiles using the PC-Mos II computer program.⁵

3. Electrochemistry

$\text{K}\{\text{Fe}(\text{DSBDC})\}\cdot 3\text{H}_2\text{O}$ was dried at $150 \text{ }^\circ\text{C}$ under vacuum overnight prior to its use in order to ensure the complete removal of water molecules. Different half-cells were prepared and $\text{K}\{\text{Fe}(\text{DSBDC})\}$ was cycled against Li, Na, or K metal electrode to investigate its electrochemical activities versus different alkali metal ions. For Li half-cells, two-electrode Swagelok®-type cells were assembled using a Li metal disc as counter and reference electrode, Whatman GF/D glass fibre as separator, and $100 \text{ }\mu\text{L}$ of LP30 electrolyte (1 M LiPF_6 in ethylene carbonate (EC):dimethyl carbonate (DMC) (1:1 vol. %) 99.9 %, from Solvionic ref. E001). The composite electrode was prepared in an Ar-filled glovebox ($\text{O}_2 < 0.5 \text{ ppm}$, $\text{H}_2\text{O} < 0.5 \text{ ppm}$) by mixing the active material with Ketjenblack® EC-600JD (KB600, Akzo Nobel) carbon conducting additive to ensure a proper electronic conduction (MOF:carbon ratio $\approx 70:30 \text{ wt}\%$, *ca.* 4 mg of active material per electrode). Self-supported electrodes were used for electrochemical testing in Na and K half-cells. Dehydrated $\text{K}\{\text{Fe}(\text{DSBDC})\}$ powder was mixed with Ketjenblack® EC-600JD (Akzo Nobel) in the 70:30 wt% ratio, then 4 wt% of polytetrafluoroethylene (PTFE, Sigma-Aldrich) was added. For Na-ion batteries, the cell was assembled with Na metal as counter electrode, 5 M NaTFSI in 1,2-dimethoxyethane (DME) as electrolyte, and a Whatman GF/D glass fibre as separator. For K-ion batteries, K metal was used as counter electrode, 5 M KTFSI in DME as electrolyte, a Whatman glass fibre GF/D disk and a tri-layer polypropylene polyethylene membrane (Celgard 2325) as separators. Coin cells (CR2032) were assembled in an Ar-filled glovebox ($\text{O}_2 < 0.5 \text{ ppm}$, $\text{H}_2\text{O} < 0.5 \text{ ppm}$). The electrochemical cells were then cycled in galvanostatic mode at various cycling rate (C/n means abusively one e^- exchanged per Fe in n hrs) starting in reduction by using a MPG-2 multi-channel system (Bio-Logic SAS, Seyssinet-Pariset, France). The electrochemical cycles are defined by an oxidation (charge) followed by a reduction (discharge), *i.e.* after the initial

reduction of the material to reach a fully alkalinated state, as commonly found in positive electrodes materials.

Table S1. Crystallographic information of $\text{K}\{\text{Fe}(\text{DSBDC})\}\cdot 3\text{H}_2\text{O}$ and $\text{K}\{\text{Fe}(\text{DSBDC})\}$.

Compound	$\text{K}\{\text{Fe}(\text{DSBDC})\}\cdot 3\text{H}_2\text{O}$	$\text{K}\{\text{Fe}(\text{DSBDC})\}$
Crystal system	Triclinic	Triclinic
Wavelength / Å	0.671415	0.64561
Space group	<i>P1</i>	<i>P1</i>
<i>a</i> / Å	3.5789(2)	3.6329(2)
<i>b</i> / Å	8.6001(7)	8.5173(1)
<i>c</i> / Å	10.407(1)	11.0922(1)
α / °	114.181(5)	131.648(5)
β / °	99.801(8)	97.128(5)
γ / °	92.103(8)	92.333(8)
<i>V</i> / Å ³	285.93(4)	250.95(5)
<i>R</i> _{wp}	0.065	0.045
<i>R</i> _{Bragg}	0.045	0.017

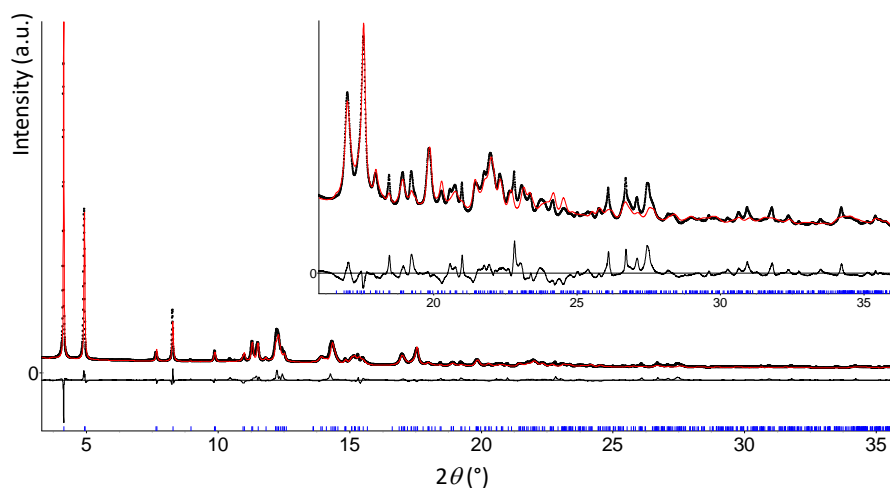


Figure S1. Rietveld plot of $\text{K}\{\text{Fe}(\text{DSBDC})\}\cdot 3\text{H}_2\text{O}$. $R_{\text{wp}} = 0.065$ and $R_{\text{Bragg}} = 0.045$ ($\lambda_{\text{synchrotron}} = 0.671415\text{Å}$).

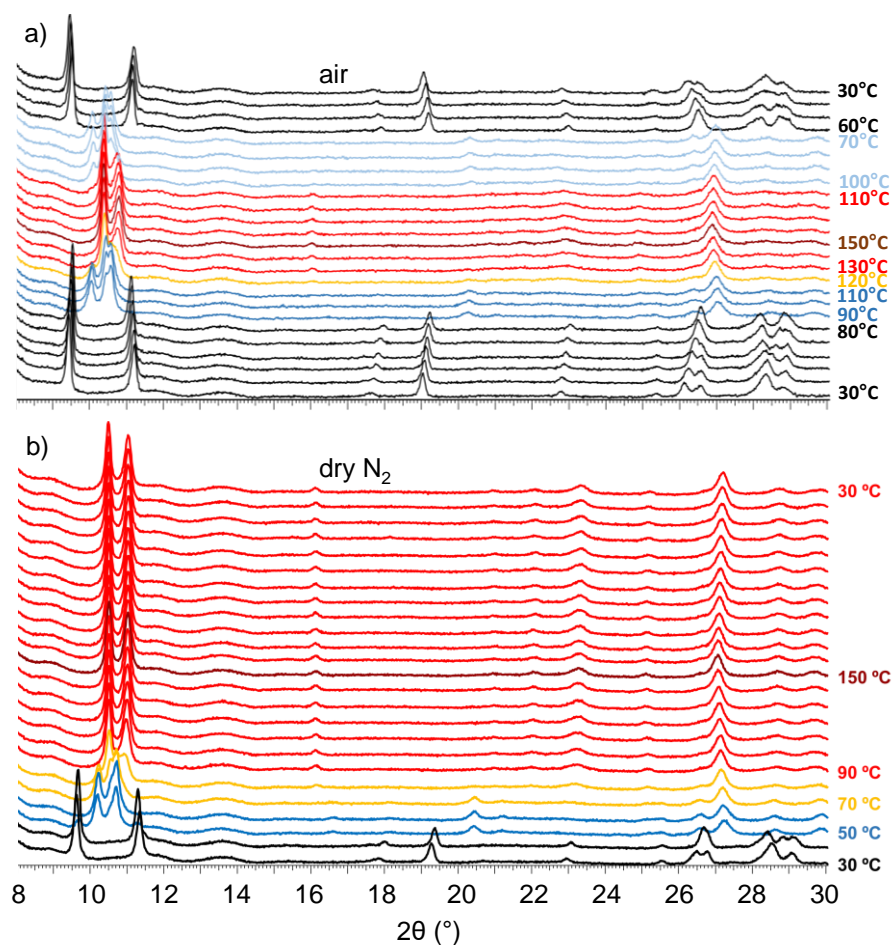


Figure S2. Temperature dependent PXRD analysis of $\text{K}\{\text{Fe}(\text{DSBDC})\}\cdot 3\text{H}_2\text{O}$ carried out a) air and b) dry nitrogen, highlighting the reversibility of the dehydration process in the presence of water vapor (heating procedure: 30 to 100–150 to 30 °C with a 10 °C step).

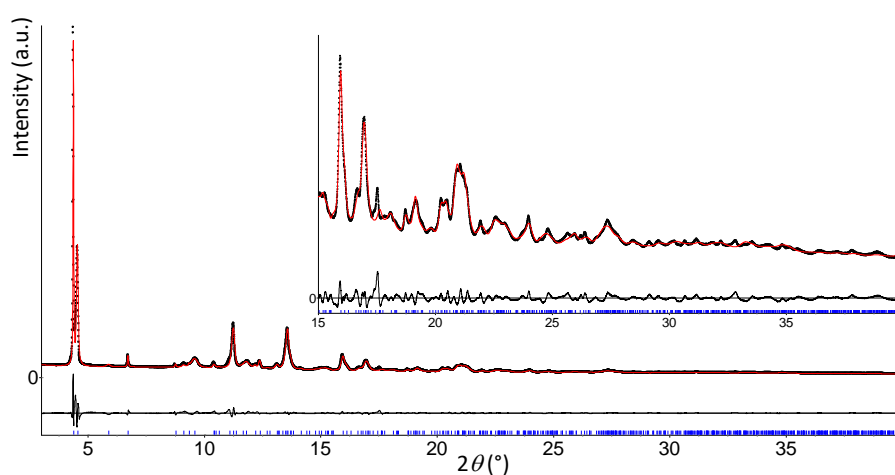


Figure S3. Rietveld plot of $\text{K}\{\text{Fe}(\text{DSBDC})\}$. $R_{\text{wp}} = 0.045$ and $R_{\text{Bragg}} = 0.017$ ($\lambda_{\text{synchrotron}} = 0.64561\text{\AA}$).

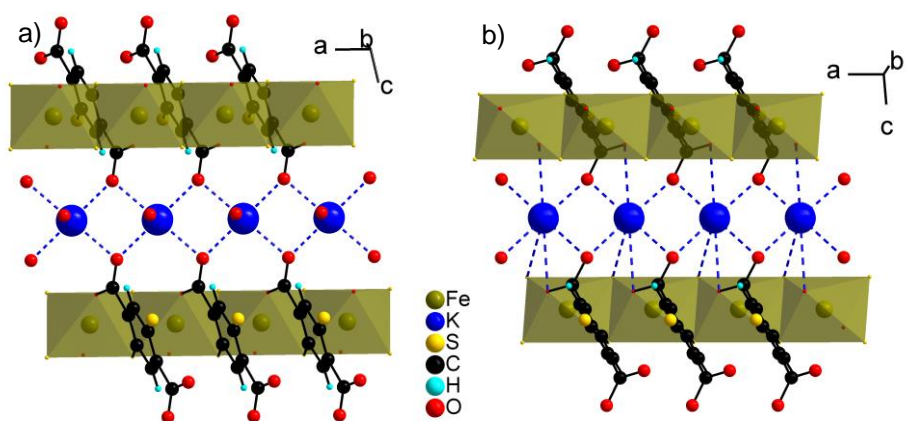


Figure S4. Comparison of the environment of the potassium ions in a) $\text{K}\{\text{Fe}(\text{DSBDC})\}\cdot 3\text{H}_2\text{O}$ and b) $\text{K}\{\text{Fe}(\text{DSBDC})\}$.

Table S2. Fe–(O,S) and K–(O,S) bond distances in $\text{K}\{\text{Fe}(\text{DSBDC})\}\cdot 3\text{H}_2\text{O}$ and $\text{K}\{\text{Fe}(\text{DSBDC})\}$.

	$\text{K}\{\text{Fe}(\text{DSBDC})\}\cdot 3\text{H}_2\text{O}$	$\text{K}\{\text{Fe}(\text{DSBDC})\}$
Fe–O	1.92(2)	1.95(5)
Fe–O	1.92(3)	1.95(5)
Fe–S	2.46(3)	2.50(3)
Fe–S	2.48(3)	2.50(3)
Fe–S	2.48(2)	2.49(3)
Fe–S	2.51(2)	2.51(3)
K–O	2.57(4)	2.47(4)
K–O	2.60(4)	2.48(3)
K–O	2.59(3)	2.59(4)
K–O	2.59(4)	2.77(4)
K–O	2.59(4) (water)	3.10(4)
K–O	2.58(4) (water)	3.16(5)
K–S	-	3.36(3)

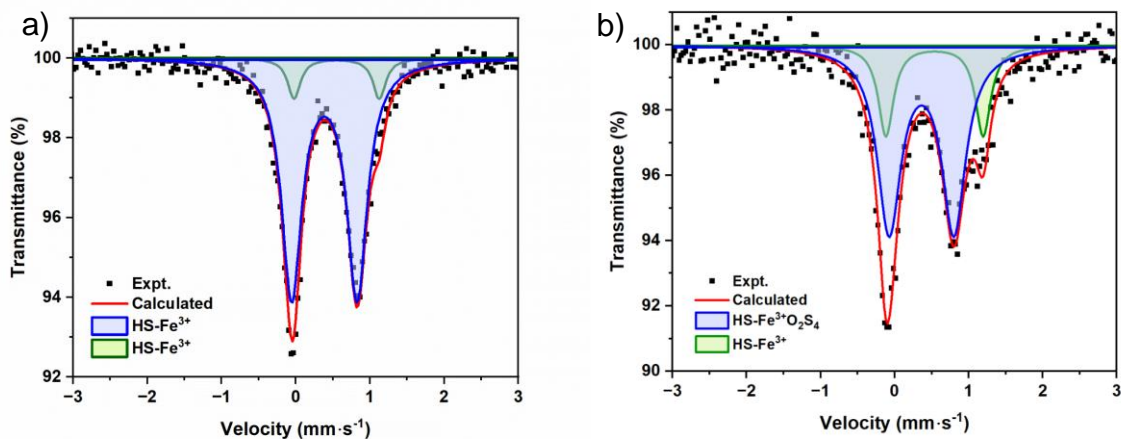


Figure S5. Mössbauer spectra of a) $\text{K}\{\text{Fe}(\text{DSBDC})\}\cdot 3\text{H}_2\text{O}$ and b) $\text{K}\{\text{Fe}(\text{DSBDC})\}$ collected at 298 K. The later was collected in the *in situ* cell but without any electrolyte.

Table S3. ^{57}Fe Mössbauer hyperfine parameters at 298 K on $\text{K}\{\text{Fe}(\text{DSBDC})\}\cdot 3\text{H}_2\text{O}$ in the pristine state and $\text{K}\{\text{Fe}(\text{DSBDC})\}$ cycled using a Leriche-type electrochemical cell.⁴

State	δ (mm s^{-1})	Δ (mm s^{-1})	Area (%)	Assignment
hydrated	0.50	0.88	90	$\text{HS-Fe}^{3+}\text{S}_4\text{O}_2$
	0.66	1.15	10	$\text{HS-Fe}^{3+}\text{O}_6$
OCV	0.47	0.87	71	$\text{HS-Fe}^{3+}\text{S}_4\text{O}_2$
	0.65	1.30	29	$\text{HS-Fe}^{3+}\text{O}_6$
middle of discharge (2.4 V)	0.43	1.30	26	$\text{HS-Fe}^{3+}\text{S}_4\text{O}_2$
	0.74	1.64	35	$\text{HS-Fe}^{3+}\text{O}_6$
	0.94	2.79	14	$\text{HS-Fe}^{2+}\text{S}_4\text{O}_2$
end of discharge (1.8 V)	1.06	2.18	25	$\text{HS-Fe}^{2+}\text{O}_6$
	0.97	2.84	75	$\text{HS-Fe}^{2+}\text{S}_4\text{O}_2$
	1.17	2.12	25	$\text{HS-Fe}^{2+}\text{O}_6$

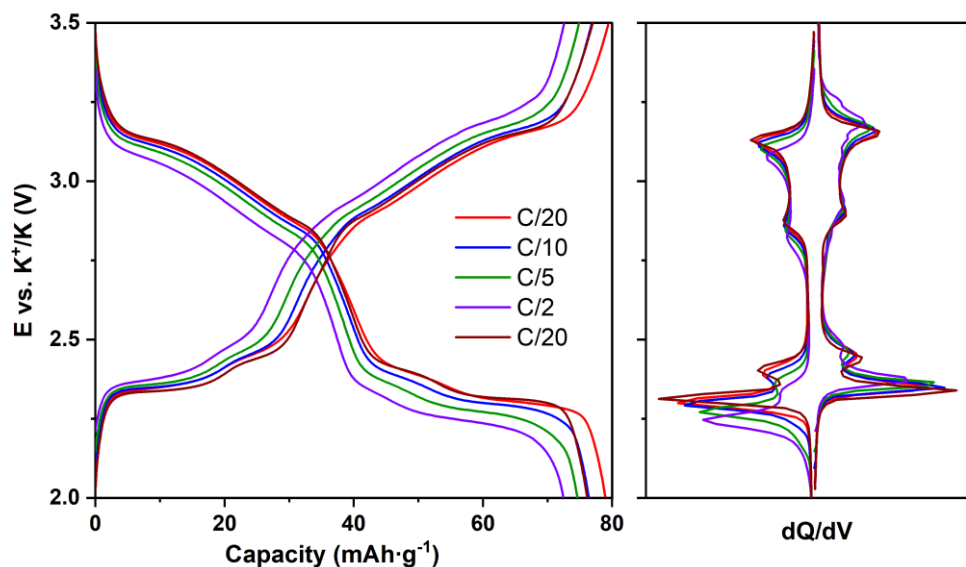


Figure S6. Overlay of the potential-capacity curves recorded at the 1st, 6th, 11th, 16th, and 20th cycles corresponding to the capability plot reported in Figure 2d.

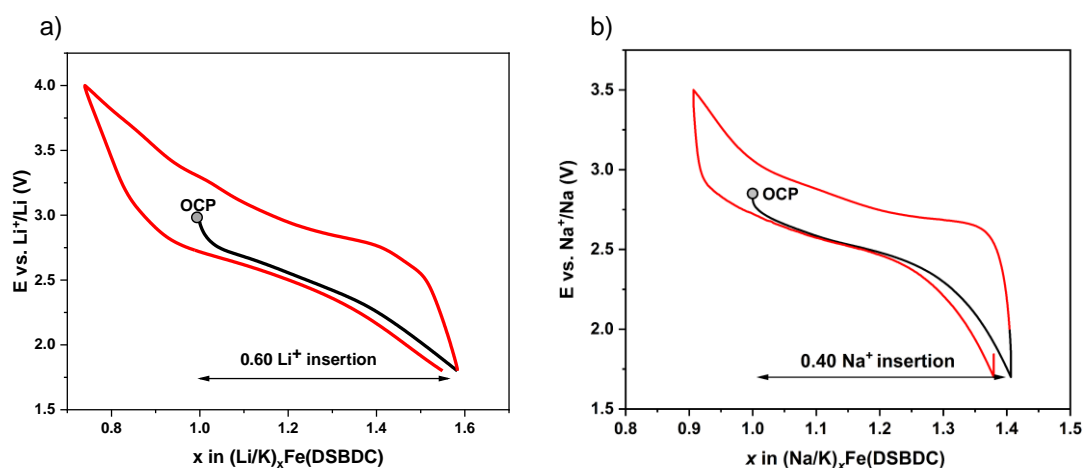


Figure S7. a) Electrochemical behaviour of $\text{K}\{\text{Fe}(\text{DSBDC})\}$ measured in Li half-cell at a cycling rate of C/10 (electrolyte: 1 M LiPF_6 in EC:DMC 1:1; potential range: 1.8–4.0 V vs. Li^+/Li). Equivalent cycling measurements performed in Na half-cell (electrolyte: 5 M NaTFSI in DME; voltage range: 1.7–3.5 V vs. Na^+/Na). Only the first and half cycle is shown.

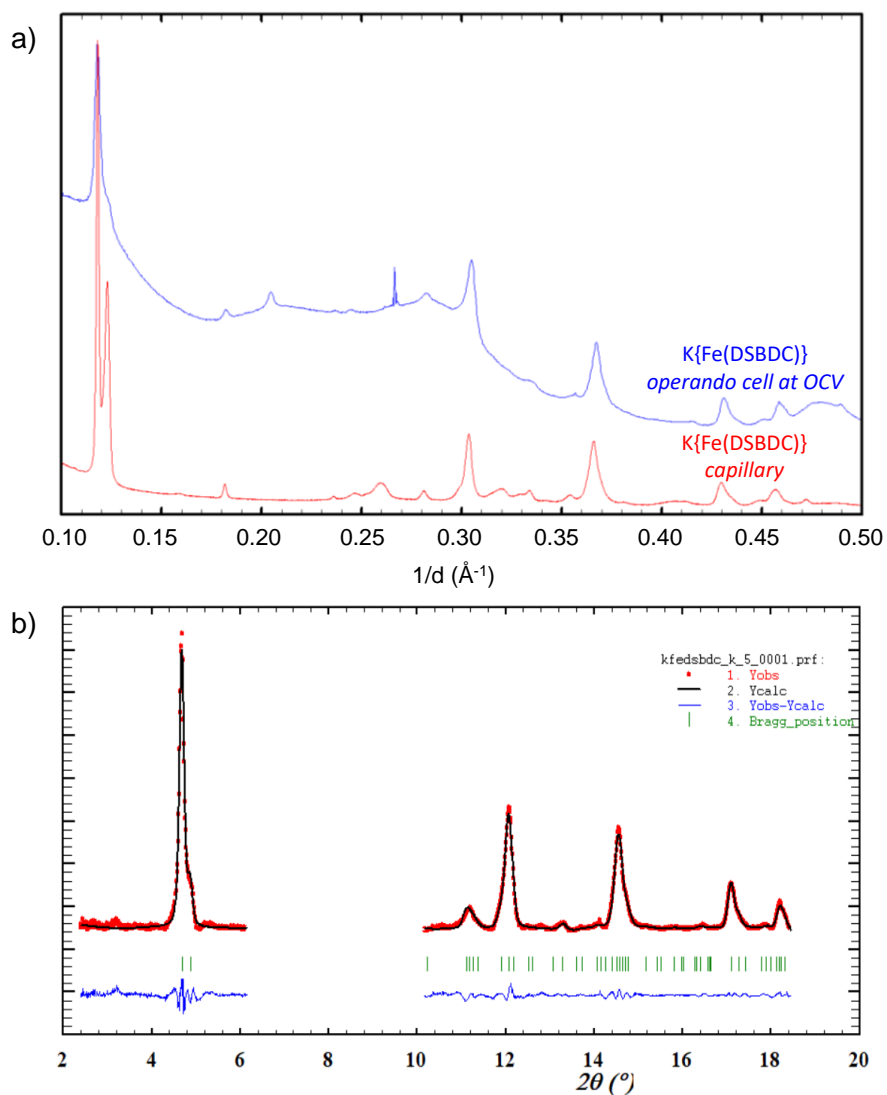


Figure S8. a) Comparison of the PXRd patterns of KFe(DSBDC) collected in a sealed glass capillary (laboratory, $\lambda = 1.5406 \text{ \AA}$) and in the *operando* cell in the presence of the electrolyte at OCV (synchrotron, $\lambda = 0.6889 \text{ \AA}$); b) "Profile pattern matching of KFe(DSBDC) at OCV in the *operando* cell using the cell parameters determined by synchrotron PXRd on a pure sample (peaks arising from other materials present in the *operando* cell have been discarded).

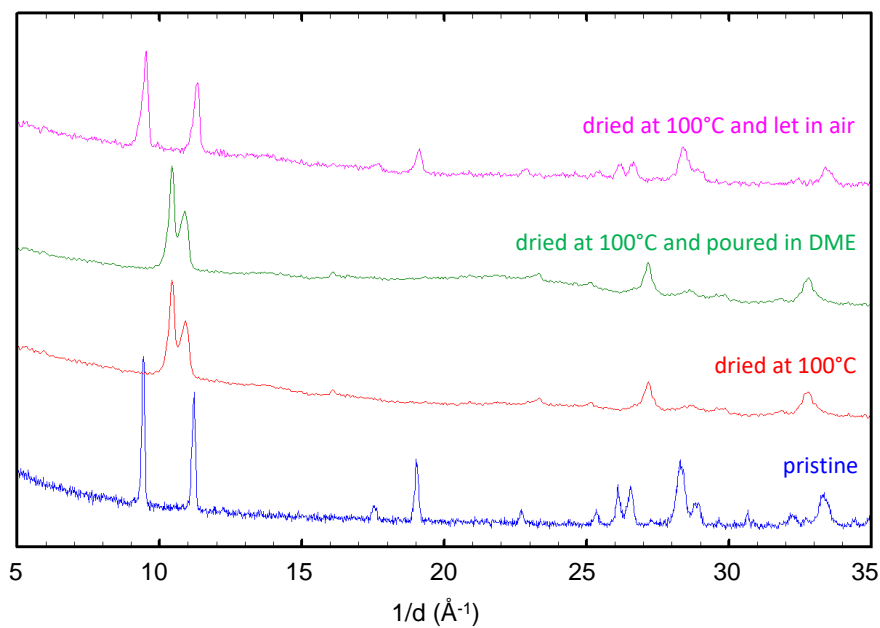


Figure S9. From bottom to top: PXRD patterns of pristine $\text{KFe}(\text{DSBDC}) \cdot 3\text{H}_2\text{O}$, $\text{KFe}(\text{DSBDC})$, $\text{KFe}(\text{DSBDC})$ poured in DME, and $\text{KFe}(\text{DSBDC})$ exposed to air ($\lambda = 1.5418 \text{ \AA}$).

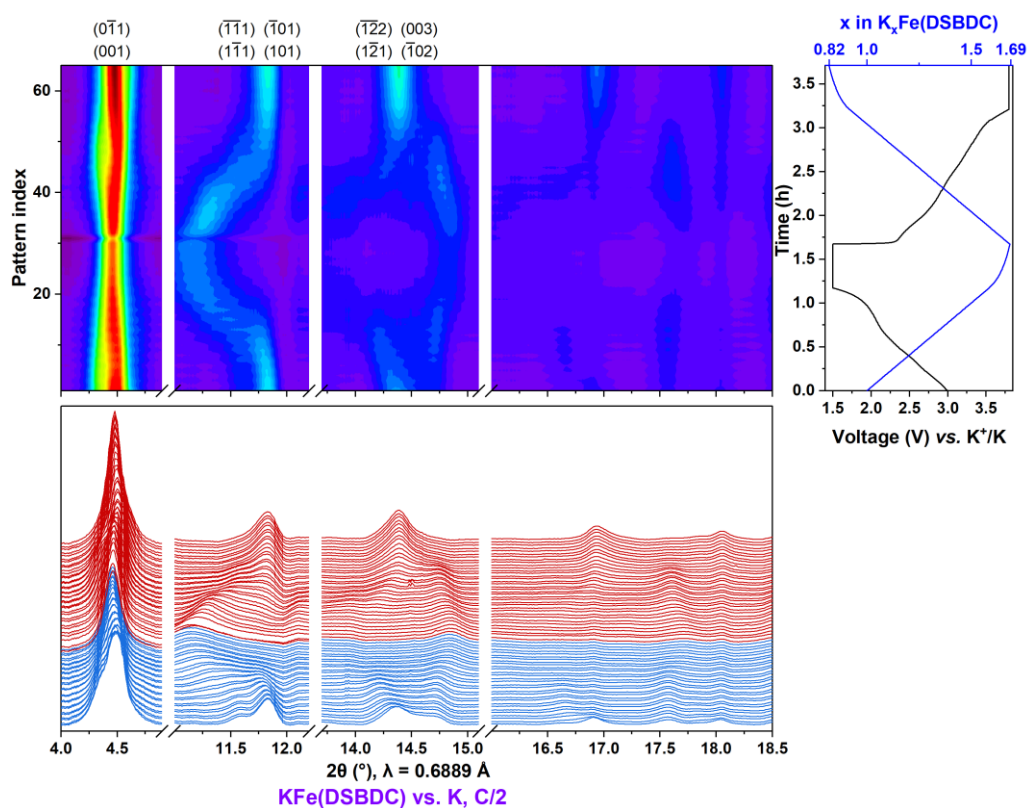


Figure S10. Operando PXRD data recorded at $C/2$ in the voltage range of 1.5–3.8 V vs. K^+/K (electrolyte 5 M KTFSI in DME); the corresponding electrochemical trace is also shown.

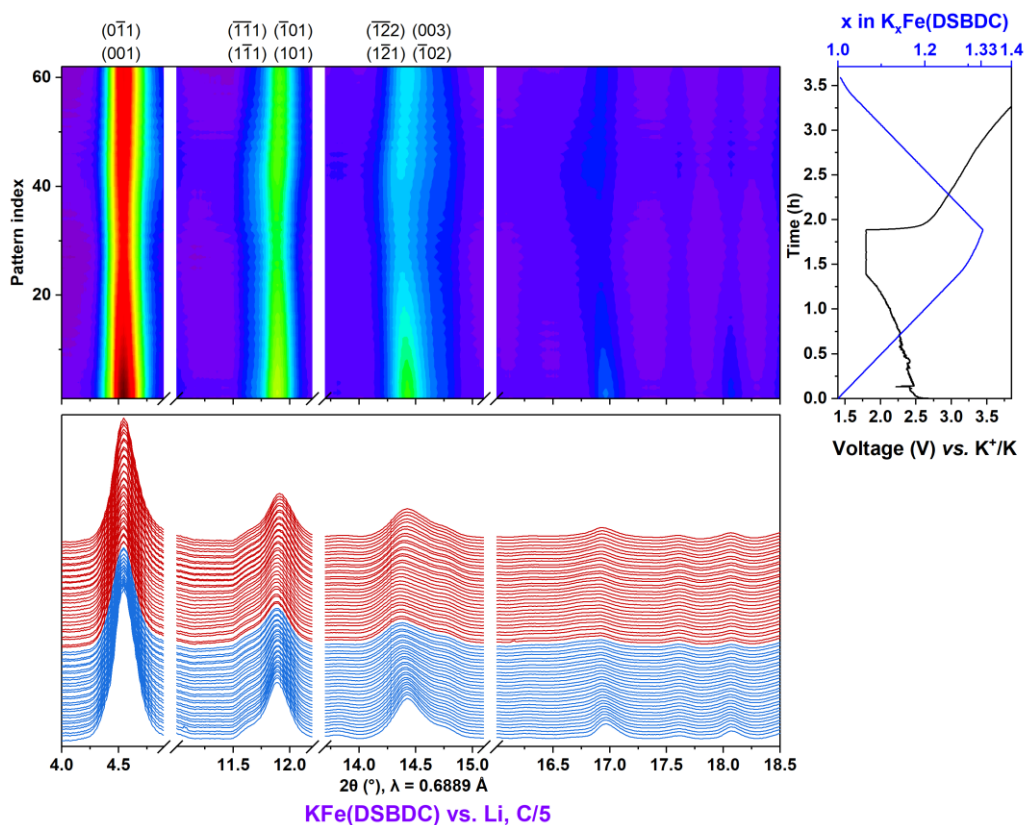


Figure S11. Operando PXRD data recorded at C/2 in the voltage range of 2.0–4.0 V vs. Li⁺/Li (electrolyte 1M LiPF₆ in EC:DMC 3:7); the corresponding electrochemical measurement is also shown.

¹ L. Vial, R. F. Ludlow, J. Leclaire, R. Pérez-Fernandez and S. Otto. *J. Am. Chem. Soc.* **2006**, 128, 10253–10257.

² N. Gedikoglu, P. Salcedo-Abraira, L. H. B. Nguyen, N. Guillou, N. Dupré, C. Payen, N. Louvain, L. Stievano, P. Poizot and T. Devic, *J. Mater. Chem. A*, **2023**, 11, 23909–23921.

³ TOPAS V5, 0: General Profile and Structure Analysis Software for Powder Diffraction Data, Bruker AXS Ltd, 1999, 2014.

⁴J.-B. Leriche, S. Hamelet, J. Shu, M. Morcrette, C. Masquelier, G. Ouvrard, M. Zerrouki, P. Soudan, S. Belin, E. Elkaim, S. Belin, E. Elkaïm and F. Baudalet, *J. Electrochem. Soc.*, **2010**, 157, A606–A610

⁵ G. Grosse, PC-Moss II, Version 1.0 Manual and Program Documentation, **1993**.